

# **Examining the Role of Wingtip Spacing in the Interaction of Two Pitching Hydrofoils**

David S. Lee<sup>1</sup> and Keith W. Moored III.<sup>2</sup>

Lehigh University, Bethlehem, Pennsylvania, 18015, USA

# John T. Hrynuk<sup>3</sup>

Army Research Lab, Aberdeen Proving Ground, MD, 21005, USA

Schooling interactions in fish have long fascinated scientists and engineers. One unresolved issue is the effect of vertical changes in swimmer relative positions in modulating hydrodynamic interactions. In this paper the spanwise relative position is tested experimentally using simple hydrofoil models. Hydrofoils in an in-line configuration undergo sinusoidal oscillations about their leading edges at a fixed frequency and amplitude. The streamwise spacing, spanwise offset, and phase relation between the hydrofoils is varied. Direct force measurements are used to investigate changes in thrust production, spanwise force, power consumption, and propulsive efficiency. The spanwise offsets tested are shown to be neutral equilibrium points in the spanwise direction. The leader hydrofoil experiences increased thrust production, power consumption, and propulsive efficiency with decreases in streamwise spacing. The leader experiences limited effects with changes in phase and spanwise offset. By modulating its phase offset the follower hydrofoil can either match or exceed the thrust generated by the leader. Increasing the spanwise offset decreases the peak power consumption and increased the efficiency of the follower hydrofoil. The follower experiences maximum propulsive efficiency for all spanwise spacings tested near  $Z^* = 0.25$  chords.

#### I. Nomenclature

A	=	Amplitude of oscillation
$\mathcal{C}_{[*]}$	=	Nondimensional coefficient for quantity [*]
S	=	Spanwise force (Newtons)
$X^*$	=	Non-dimensional streamwise offset
$Z^*$	=	Non-dimensional spanwise offset
$\theta_0$	=	Oscillation amplitude (Degrees)
$\theta$	=	Instantaneous pitch angle (Degrees)
AR	=	Aspect Ratio
P	=	Power consumption (Watts)
Re	=	Reynolds number
St	=	Strouhal number
T	=	Thrust (Newtons)
U	=	Freestream velocity (Meters per second)
b	=	Span (Meters)
С	=	Chord (Meters)
f	=	Dimensional frequency (Hertz)
k	=	Reduced frequency

<sup>&</sup>lt;sup>1</sup> Graduate Student, Department of Mechanical Engineering and Mechanics, AIAA Student Member.

<sup>&</sup>lt;sup>2</sup> Associate Professor, Department of Mechanical Engineering and Mechanics, AIAA Member.

<sup>&</sup>lt;sup>3</sup> Research Mechanical Engineer, DEVCOM - ARL, AIAA Member.

t = Time (Seconds)  $\eta$  = Efficiency (Percentage)  $\nu$  = Kinematic Viscosity (Meters squared per second)  $\rho$  = Density (Kilograms per cubic meter)  $\phi$  = Phase offset (Degrees)

## II. Introduction

Schooling interactions are of interest for understanding the potential gains in efficiency and performance for individual swimmers as well as collective performance of the schooling group [1]. This has practical applications for real world engineering challenges such as swarming unmanned aerial and underwater systems. By tailoring their positioning and kinematics biological swimmers may achieve higher efficiencies than would be possible in isolation [2]. Significant work has already been done on schooling interactions [3-5]. However, the role of the tip vortex system from three-dimensional hydrofoils has been largely unexplored. A finite span hydrofoil producing lift will shed a vortex from each of its tips, affect nearby swimmers. This study investigates the three-dimensional effects on schooling interactions experimentally, specifically the interaction of a leader's tip vortex system with a follower.

Wing tip vortex interactions are common in birds and aircraft flying in formation. In tight formations one lifting surface may interact with the tip vortex systems of one or several other lifting surfaces. This type of steady flow interaction is also observed in nature where, for instance, gliding pelicans will position themselves in a V formation to increase their glide distance [17]. A following aircraft in a formation flight can potentially take similar advantage of the vortices shed by a leader aircraft to reduce drag. However, if the following pilot miscalculates their positioning, they may experience potentially catastrophic adverse effects (such as the ingestion of highly turbulent air into an engine). A thorough understanding of these interactions is thus vital.

Tip vortex systems take the form of streamwise vortices whose axes of rotation are aligned with the free stream [6]. The continuous interaction of streamwise vortices with finite span translating wings has received attention with previous research studies [7-9]. These studies showed that the spanwise location at which the incident vortex impinged on a finite wing greatly impacted the interaction between the incident vortex and the tip vortex system of the wing. In cases where the impinging vortex is outboard of the wingtip, the vortices pair up and propel themselves upwards and away from the wing. In cases where the two vortices were directly aligned with one another there is strong interaction between the feeding shear layers for each vortex. While both vortices maintain coherent cores in the time averaged flow field, they dissipated in the wake due to the induced instabilities in their feeding shear layers. Finally, for the case of inboard positioning, the impinging vortex experiences a spiral instability as it approaches the wing bifurcating when it hits the leading edge of the wing. The impinging vortex induces a downwash on the wing which acts to reduce the effective angle of attack, reducing the strength of the wing's tip vortex system. All cases saw significant unsteady loading and alterations to the mean aerodynamics forces acting on the wing.

The addition of dynamic motion, such as heaving causes structural modification of a trailing vortex system shed by a wing as documented by Fishman [10]. For a finite wing undergoing slow oscillatory heaving the induced undulations in the shed vortex resulted in large variations in axial velocity and circulation. Orbital motion of the tip vortex also occurred where vortex core motion was observed in the spanwise direction in addition to the forced motion in the heaving direction. These orbital motions of the vortex generally appeared for higher Strouhal number [10], defined as:

$$St = fA/U \tag{1}$$

Where f is the dimensional heaving or oscillating frequency, A is the amplitude of oscillation (peak-to-peak), and U is the freestream velocity.

When these slowly heaving wings interact with an impinging streamwise vortex the interaction becomes intermittent. These interactions are, like the continuous cases mentioned previously [7-9], highly dependent on the spanwise impingement location. For example, when the incident vortex impinges inboard of the wingtip it induces a downwash which acts to reduce the effective angle of attack of the wing, reducing the strength of the wing's tip vortex. The strength of this downwash is also dependent on the point in the heaving cycle in which the wing interacted with the incident vortex [11]. Vortex-body interactions similar to these are commonly observed in biological schooling and formation flight in birds. Another landmark study found that ibises fly in optimal V formation positioning predicted

by steady aerodynamic theory. Moreover, they synchronize their flapping phase to take advantage of the upwash/downwash interactions from leaders in the flock [18]. This suggests a deliberate exploitation of an unsteady flow interacting with a lifting surface to increase aerodynamic performance in nature. Replicating this in man-made devices is a driving motivation for the current work.

Another common situation is fish swimming in schools. [Fish will school for a variety of reasons including socialization, predator avoidance and feeding [12-15]. Of interest here is the evidence that orderly positioning of swimmers, analogous to those mentioned for birds, can lead to hydrodynamic benefits collectively for the school as well as for individual swimmers [16]. A key extension to this question is whether some formations are more advantageous compared to others. Efforts have been made to establish canonical schools as test beds to probe the hydrodynamics of multiple swimmer interactions. An example of an early attempt was by Weihs who proposed a simple diamond pattern school model [16]. This model, while still sometimes used as a starting point, has been found to not be particularly representative of natural schooling interactions [14]. Further developments have led to the current framework used to study the interaction of simplified propulsors, represented by hydrofoils, based on the orientation of the leading edges relative to one another [3-5], which is used in the current study. This study focuses on what is referred to as an in-line configuration where one hydrofoil, the leader, is directly in front of another, the follower, see Fig. 1 (b). Most commonly the hydrofoils used in this framework have a sinusoidal oscillation profile about their leading edge defined by:

$$\theta_{Leader}(t) = \theta_0 \sin(2\pi f t) \tag{2a}$$

$$\theta_{Follower}(t) = \theta_0 \sin(2\pi f t + \phi)$$
 (2b)

Where  $\theta_0$  is the amplitude of oscillation, f is the oscillating frequency, and t is time. The phase offset ( $\phi$ ) is the difference between the two hydrofoils in their oscillating cycles. A phase value of  $\phi = 180^{\circ}$  would mean that the hydrofoils were completely out of phase (i.e. when one propulsor was fully pitched up, the other is fully pitched down).

Studies on the performance of two-dimensional oscillating hydrofoils in the in-line configuration have proven to be informative first steps. One study showed that by varying the phase of oscillation and streamwise spacing between two oscillating foils generated significant improvements in the efficiency, in some cases upwards of 150% [3]. However, the effects on the leading foil were limited except for cases where the leader and follower were close (less than one chord length). In cases where the follower produced larger amounts of thrust the time average flow field showed a single, high momentum, jet being shed in the freestream direction. This directed most of the momentum added to the flow in the free-stream direction creating useful thrust. Cases with lower performance exhibited a branched wake, with two jets produced at oblique angles to the free stream where a significant portion of the momentum added to the flow is lost to the cross-stream direction.

While informative, infinite span studies do not always accurately depict real word swimmers. Finite and infinite span hydrofoils have been shown to give very different results. For the in-line case an opposite trend in propulsive efficiency was observed when finite span hydrofoils were used [5]. The optimal spacing and phase, which generated the greatest propulsive efficiency for infinite span hydrofoils, resulted the lowest propulsive efficiency when applied to finite span hydrofoil cases. This suggests that the tip vortex system present in finite span hydrofoils plays a major role. By varying the spanwise offset of oscillating hydrofoils, the effect of the three-dimensional tip vortex system can be probed experimentally.

# III. Experimental Methods

#### A. Experimental setup

Oscillating finite span hydrofoils have been constructed with the ability to vary their positioning relative to one another in the spanwise and streamwise directions. High resolution six-axis ATI Nano 43 force transducers were used to measure the hydrodynamic forces acting on each hydrofoil. In this study the two hydrofoils were placed in the inline configuration, see Fig. 1, and will be referred to by their placement, with the "leader" being upstream of the "follower". An acrylic plate was mounted over the water surface to mitigate free-surface effects. A traverse system powered by a stepper motor facilitated automated changes to the spanwise offset between the hydrofoils. The tips of the hydrofoils were kept at least one chord from the top and bottom of the tunnel. High torque servo motors directly

controlled the pitch angle of each hydrofoil and high resolution optical encoders were used to record angular position data.

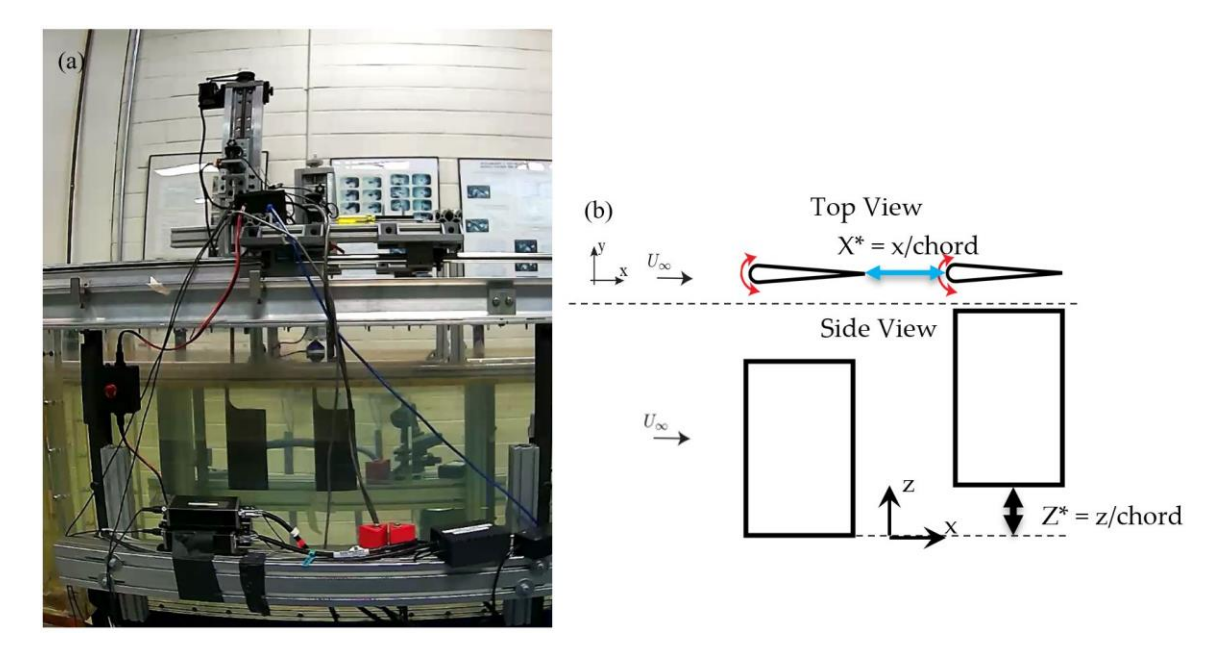


Fig. 1 (a) Photograph and (b) Simplified schematic of experimental setup

The hydrofoils were manufactured using a fused deposition modeling (FDM) 3D printer and sanded smooth. Both foils have a rectangular planform with a chord length of c = 9.5 cm and span of b = 19 cm giving an aspect ratio of ratio AR = b/c = 2. The cross section of the hydrofoil is a NACA 0012 airfoil shape with squared wing tips, except where mounting modifications were required. The hydrofoils were connected to the actuation mechanism with 10 mm carbon fiber rods, with the point of actuation being 5 mm behind the leading edge (approximately 5% of the chord). The leader hydrofoil was moved in the spanwise direction and was thus constructed with a longer mounting rod. To isolate the propulsive forces acting on the foils, fairings were constructed around the connecting rods with care being taken to avoid contact interference with the hydrofoils. These fairings served to shield the rods from the imposed flow thereby eliminating their drag and, consequently, isolating the forces acting on a hydrofoil itself. Data acquisition was conducted using a National Instruments PCI system operating at a sampling frequency of 1000 Hz. To capture all forces acting on the hydrofoils, the force transducers are tared in quiescent flow.

#### **B.** Parameters and variables

The hydrofoils were sinusoidally oscillated at fixed frequency and amplitude with varying phase offsets as given in Eq. (2a). The amplitude and frequency were fixed at  $\pm 7.5^{\circ}$  and 1 Hz respectively. The chord length of the hydrofoils was used as the reference length scale and the free stream velocity was set to U = 0.1 meters per second. These conditions resulted in a Reynolds, Strouhal number, and reduced frequency in the current study of Re = Uc/v = 10,000 where v is kinematic viscosity, St = 0.25, and k = fc/U = 1 respectively. Summaries of experimental parameters and variables are given in Table 1 and Error! Reference source not found., respectively.

Table 1 Experimental parameters.

Parameters				
Foil Profile	AR	St	Re	k
NACA0012	2	0.25	10,000	1

Table 2 Experimental variables.

Variable	Phase offset $(\phi)$	Streamwise spacing $(X^*)$	Spanwise offset $(Z^*)$
Range	0° to 360°	0.75 to 1.125	0 to 1
Increment	15°	0.125	0.125

Four metrics for performance will be presented for each hydrofoil: the force acting in the spanwise direction, the useful thrust produced, the power consumed, and the propulsive efficiency. Nondimensional performance coefficients are given as:

$$C_S = S/0.5\rho bcU^2 \tag{3}$$

$$C_T = T/0.5\rho bcU^2 \tag{4}$$

$$Cp = P/0.5\rho bc U^3 \tag{5}$$

$$\eta = C_t / C_P \tag{6}$$

The time-averaged spanwise force exerted on the foil (S) was normalized to the spanwise force coefficient ( $C_S$ ). The time-averaged thrust produced by the pitching motion (T) is normalized to the thrust coefficient ( $C_T$ ). The time-averaged power consumed to oscillate the hydrofoil (P) is normalized to the power coefficient ( $C_T$ ). The propulsive efficiency ( $\eta$ ) is the ratio of the thrust and power coefficients. These performance metrics are presented as time averages of six trials each consisting of 50 oscillating cycles for a total of 300 oscillating cycles for each configuration tested.

# C. Isolated Performance

To verify the functionality of the experimental setup, data was taken for both the leader and follower hydrofoils in isolation, representing how they would perform if infinitely far apart. These results are compared with those from previous studies. This isolated performance data is given in Table 3. The thrust produced by both foils aligns well with previous studies. The power consumption was notably lower than previous studies resulting in higher propulsive efficiency. This difference may be attributed to the addition of fairings around the connecting rods, a higher Reynolds number than previous work, as well as the use of a different profile shape.

Table 3 Isolated performance of leader and follower hydrofoils compared with previous studies.

Study	Re	Profile	$C_T$	$C_P$	η
2D Boschitsch (2014)	4700	Teardrop	0.150±0.020	$0.660\pm0.060$	22±4%
2D Kurt (2018)	4800	Teardrop	$0.140\pm0.050$	$0.770\pm0.001$	18±6%
2D Kurt (2018)	7500	Teardrop	0.150±0.020	0.790±0.003	19±2%
3D Kurt (2018)	7500	Teardrop	0.210±0.020	0.750±0.005	28±3%
3D Present Study, Leader, max depth	10,000	NACA0012	0.141±0.010	$0.420\pm0.002$	33±3%
3D Present Study, Follower	10,000	NACA0012	0.136±0.003	0.423±0.001	32±1%

## IV. Results and Discussion

The hydrofoils were tested in the in-line configuration with varying spanwise offset  $(Z^*)$ . The spanwise forces exerted on the hydrofoils for the nearest  $(X^* = 0.75 \text{ chords})$  and furthest  $(X^* = 1.125 \text{ chords})$  streamwise spacings can be seen in

Fig. 2. The spanwise forces on both hydrofoils for both spacings were small relative to other hydrodynamic forces acting on them. This trend was consistent for all spacings tested. These results suggest that the spanwise offsets tested are all neutral equilibrium points in the spanwise direction. That is to say, the spanwise hydrodynamic forces did not act to push or pull the hydrofoils in any particular spanwise direction. One important feature was that as the streamwise spacing decreased the variability of the hydrodynamic forces increased, caused by stronger interactions between the hydrofoils. This resulted in higher standard deviations in the performance metrics.

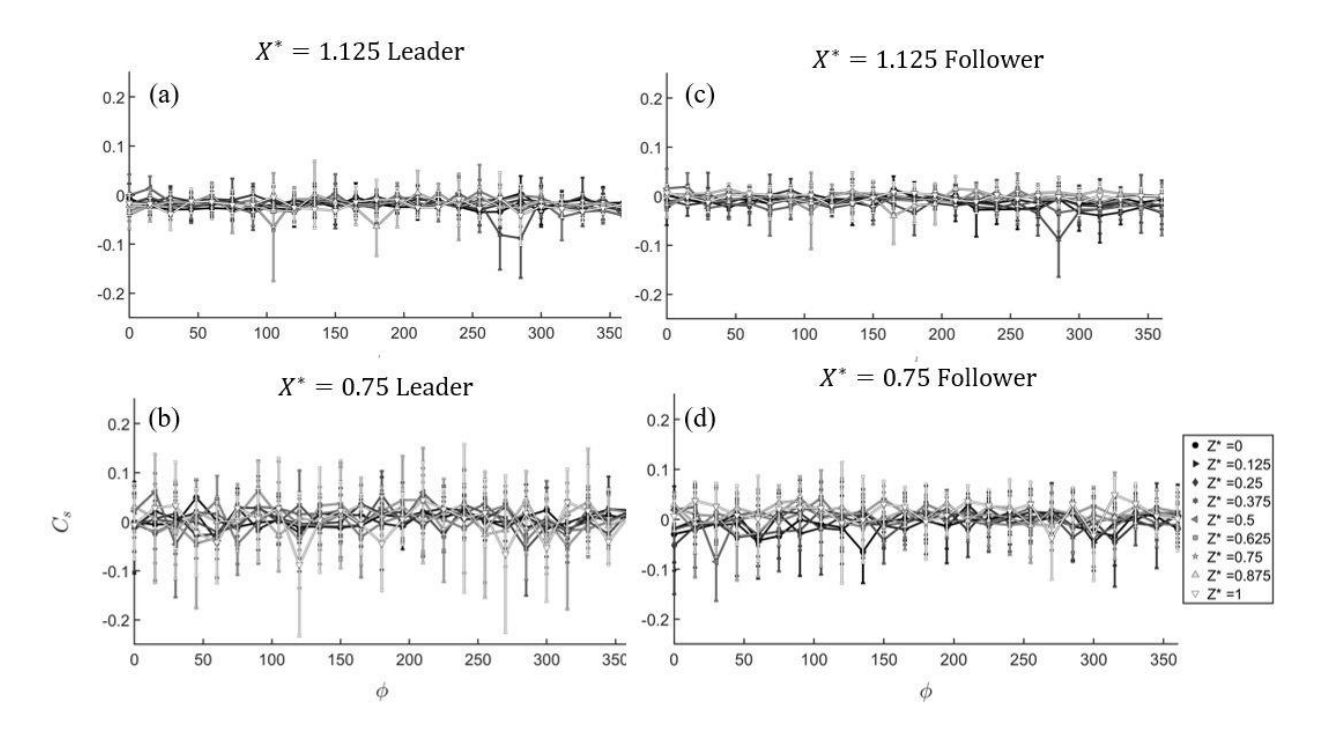


Fig. 2 Spanwise force coefficients on leader (a, b) and follower (c, d) hydrofoils for selected streamwise spacings.

When evaluating the thrust generated by the leader hydrofoil for the farthest streamwise spacing, shown in Fig. 3 (a), it exhibited no significant change from the isolated value given in Table 3. The follower, Fig. 3 (b), experienced major changes in thrust production with phase modulation relative to the leader, with a clear minima and maxima present. Increasing the spanwise offset generated a small decrease in the peak thrust produced by the follower, shown by the arrow in Fig. 3 (b). Another notable feature is that the minimum thrust produced by the follower closely matched the thrust produced by the leader, shown by the dashed line in Fig. 3. This suggests that in an unconstrained situation, where the hydrofoils could freely move up or downstream, a constant streamwise spacing would be primarily obtained through selection of relative phase with limited effects of relative spanwise location.

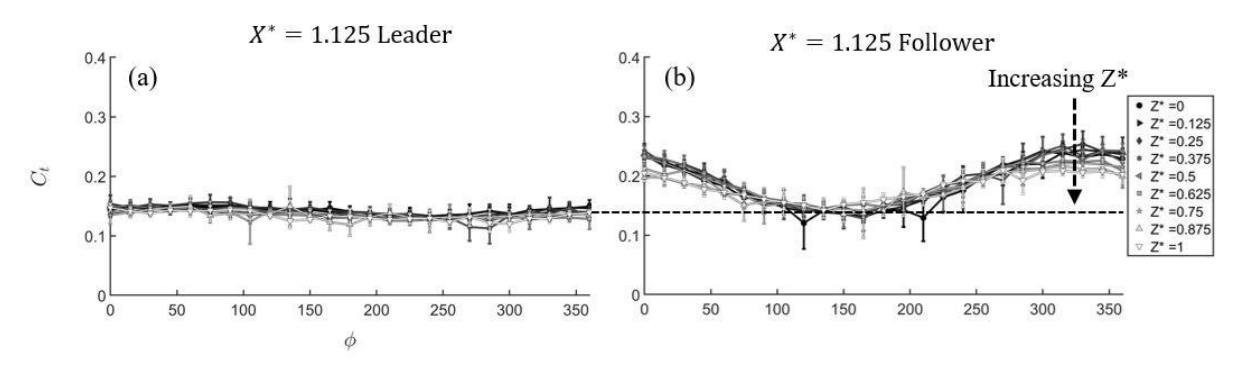


Fig. 3 Thrust coefficients for leader (a) and follower (b) hydrofoils at select streamwise spacing.

Fig. 4 shows the thrust coefficient for all the cases tested with contours of thrust coefficient for various phase shifts and spanwise offsets. As the streamwise spacing was decreased the thrust produced by the leader foil,

Fig. 4 (a-d), increased with low dependence on changes in phase and spanwise offset. The follower,

Fig. 4 (e-h), also produced slightly more thrust as the hydrofoils were moved closer together. Similar to the results observed in Fig 3, the follower data exhibits sinusoidal peaks and troughs in thrust coefficient as a function of phase

shift, again with a somewhat limited effect of spanwise offset. The clearly observable trough present at larger spacing, Figs Fig. 3 (b) and

Fig. 4 (e), became notably less apparent as the streamwise spacing decreased. Decreasing streamwise spacing also reduced the amplitude between the minimum and maximum thrust produced by the follower foil. A notable observation is the phase shift in the sinusoidal peaks and troughs observed in Fig. 3 (b) and

Fig. 4 (e-h). This shift is believed to be a function of the convective speed of the coherent vortex structures wake, and thus physically moving the models in a streamwise direction alters the relevant phase to generate maxima or minima in the thrust.

For all streamwise spacings tested the maximum thrust production by the follower hydrofoil, near double that of the isolated case, appeared to occur near the  $Z^* = 0.25$  chords. While the minimum thrust generated by the follower occurred at different spanwise offsets, this minimum thrust closely matched the thrust produced by the leader foil. This suggests that no configuration, in the parameter space probed, would result in either hydrofoil producing less time averaged thrust than if they were operating an infinite distance apart.

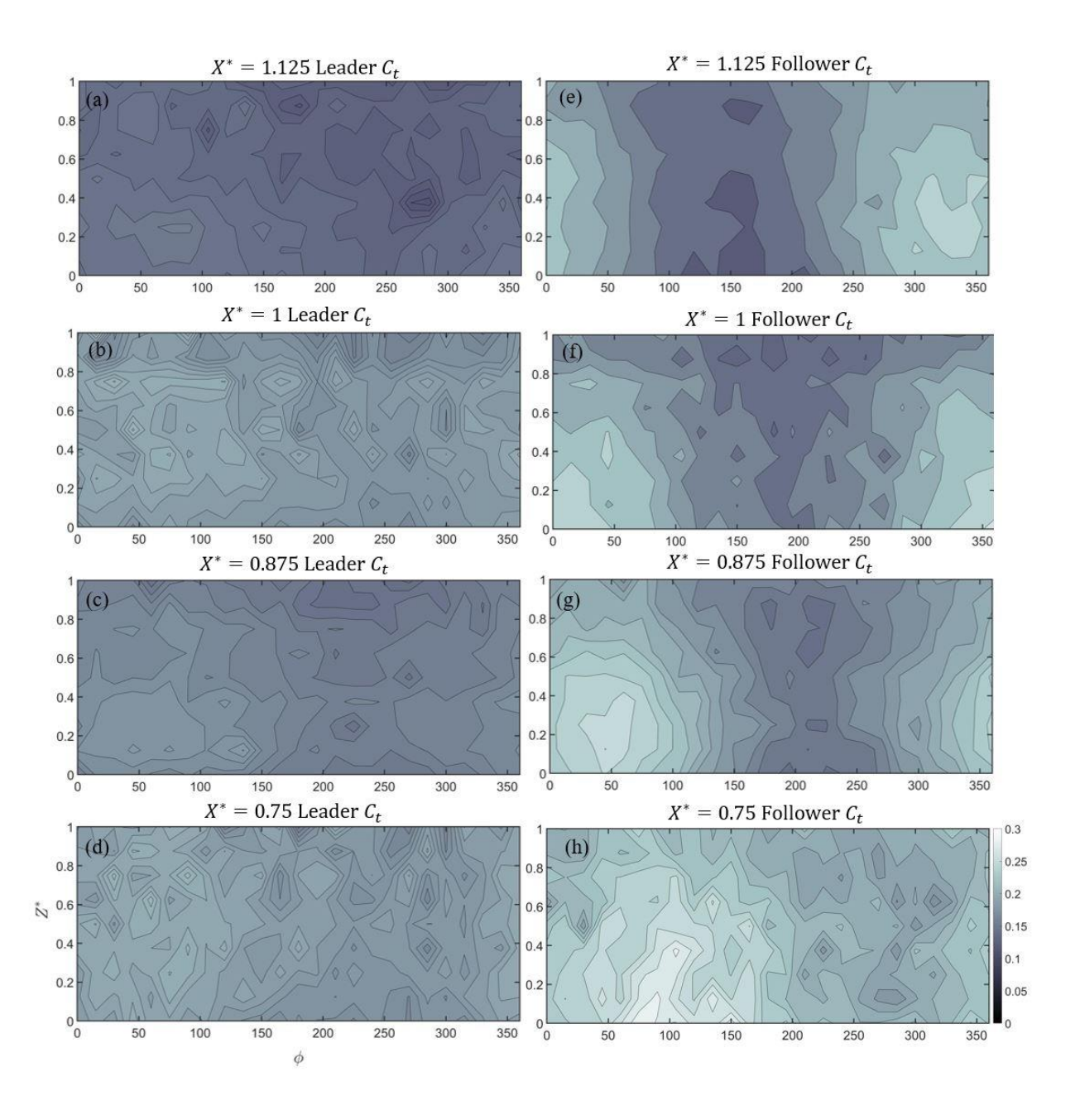


# Fig. 4 Contour plots of thrust coefficients for leader (a to d) and follower (e to h) hydrofoils

Power consumption of the hydrofoils for a select streamwise spacing,  $X^* = 1.125$ , is shown in Fig. 5. Similar to the thrust plots there are clear minima and maxima in power consumption for the follower. However, the power consumed by the leader is also affected by the relative phase of the motion. Both hydrofoils' power consumption showed sinusoidal behavior with minima near  $\phi = 185^{\circ}$  and maxima near  $\phi = 15^{\circ}$ . Here the spanwise offset had a more significant effect than for the thrust generation. The power consumption of the leader, Fig. 5 (a), was inversely proportional to increases in the spanwise offset but the effect was generally small and acted uniformly across all phases. Power consumption for the follower exhibited a more significant difference between maximum and minimum power. Unlike the uniform reduction in power consumption for the leader, increasing the spanwise offset appeared to reduce the peak and trough amplitude of the follower's power consumption curve. Therefore, increased spanwise spacing appears to have a curve flattening effect on the follower. This may be situationally beneficial or detrimental to the follower. For example, for  $\phi = 185^{\circ}$  follower power can be minimized in a purely in-line configuration ( $Z^* = 0$ ). However, if  $\phi = 15^{\circ}$  then maximizing the spanwise spacing ( $Z^* = 1$ ) serves to minimize follower power by approximately 10% over the pure in-line case.

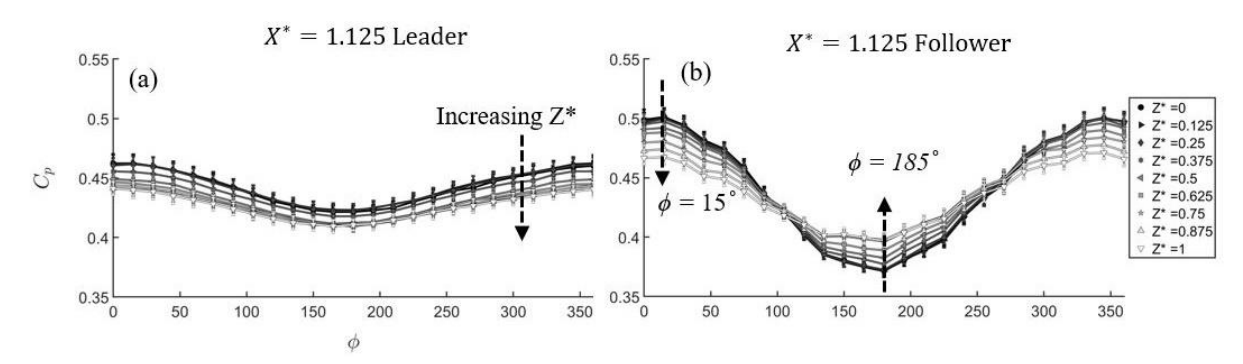


Fig. 5 Power coefficients for leader (a) and follower (b) hydrofoils at select streamwise spacing.

Figure Fig. 6 shows the contours of power coefficient ( $C_P$ ) for all the cases tested. These results show that decreasing the streamwise spacing generally increased the minimum power consumption by both hydrofoils. The phase dependence of the leader, Fig. 6 (a-d), did not shift with decreasing streamwise spacing with minima consistently occurring near  $\phi = 185^{\circ}$  and maxima near  $\phi = 15^{\circ}$ . The follower experienced trends consistent with those observed in the thrust in Fig.

Fig. 4 (e-h), where the minimum power was a function of both phase and streamwise spacing ( $X^*$ ). The maximum follower power consumption consistently occurred near  $Z^* = 0.25$  chords of spanwise offset. The sine-wave-like shape of the power consumption by the follower hydrofoil experienced a phase shift with changing streamwise offset similar to that seen in thrust production. A notable difference between the thrust and power curves is that follower's power consumption falls below that of the leader in a number of cases.

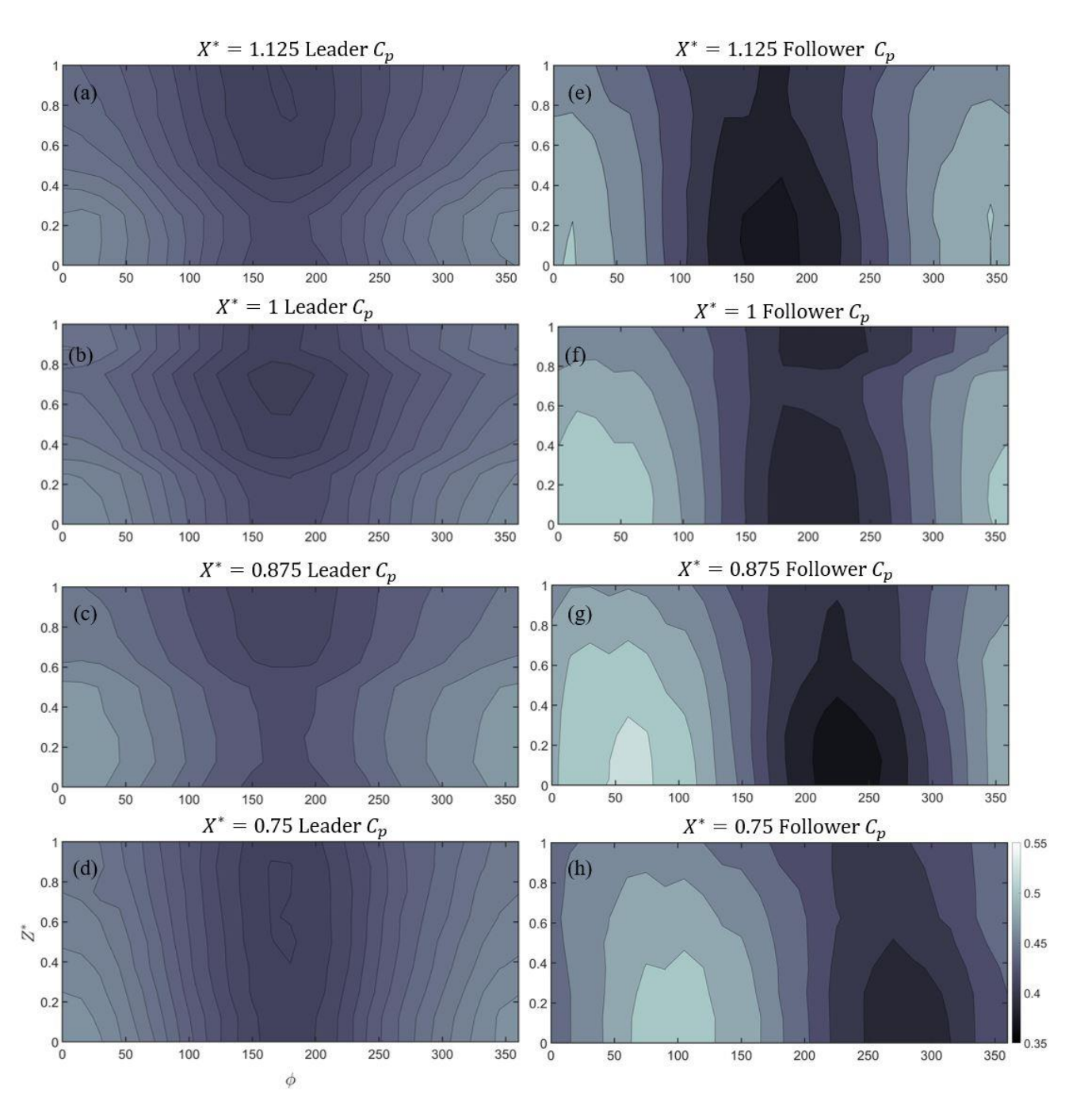


Fig. 6 Contour plots of power coefficients for leader (a-d) and follower (e-h) hydrofoils

The effect of the difference between the thrust and power trends is more clearly observed in the propulsive efficiency of the hydrofoils. Fig. 7 shows the propulsive efficiency for a select streamwise spacing of  $X^* = 1.125$ . The efficiency of the leader, Fig. 7 (a), was very close to the isolated case, see dashed line in Fig. 7. The minor changes present, less than 5%, are due to the previously identified trends in the leader power consumption in Fig. 5 (a). The follower, Fig. 7 (b), showed more drastic changes in propulsive efficiency consistent with the trends identified in the thrust and power, Fig. 3 and Fig. 5 (b). The follower's propulsive efficiency showed relatively small, less than 10%, drop in peak value with increased spanwise offset.

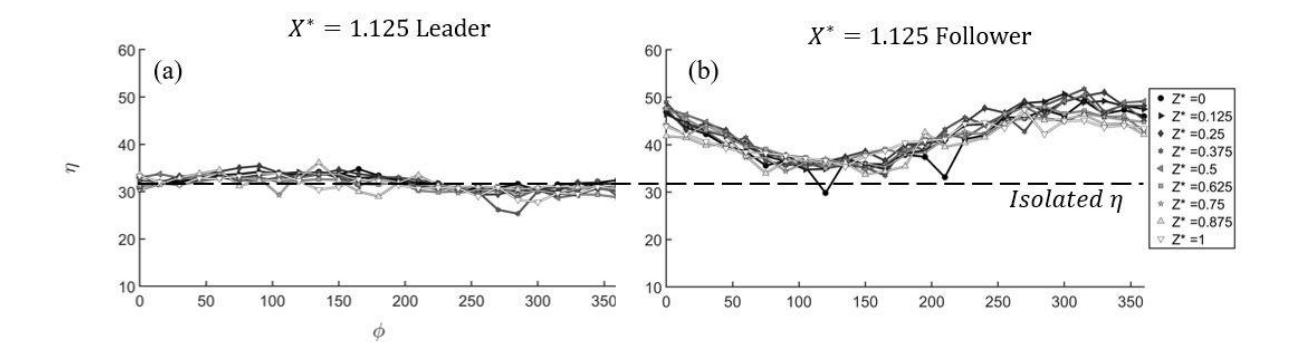


Fig. 7 Efficiency for leader (a) and follower (b) hydrofoils at select streamwise spacing.

The contours of the propulsive efficiency of both hydrofoils for all cases tested are shown in Fig. 8. Both hydrofoils follow similar trends to those seen in thrust. The leader, Fig. 8 (a-d), experienced an increase in propulsive efficiency despite the increase in power consumption. This suggests that in an in-line schooling situation both leader and follower swimmers are likely to enjoy enhanced performance across a variety of spanwise offsets. The follower, Fig. 8 (e-h), experienced more pronounced changes in efficiency which appeared to be dominated by the trends in thrust production. The follower efficiency never falls below that of the leader and stayed consistently above that of the isolated case given in Table 3. Additionally decreasing the streamwise spacing ( $X^*$ ) flattened the sinusoidal shape of the follower efficiency in a similar manner observed in the thrust production. Finally, the follower efficiency reflected both the thrust and power curves with decreasing streamwise spacing causing an increase in the phase of minimum and maximum efficiency. The maximum efficiency for the follower is again found near  $Z^* = 0.25$  chords.

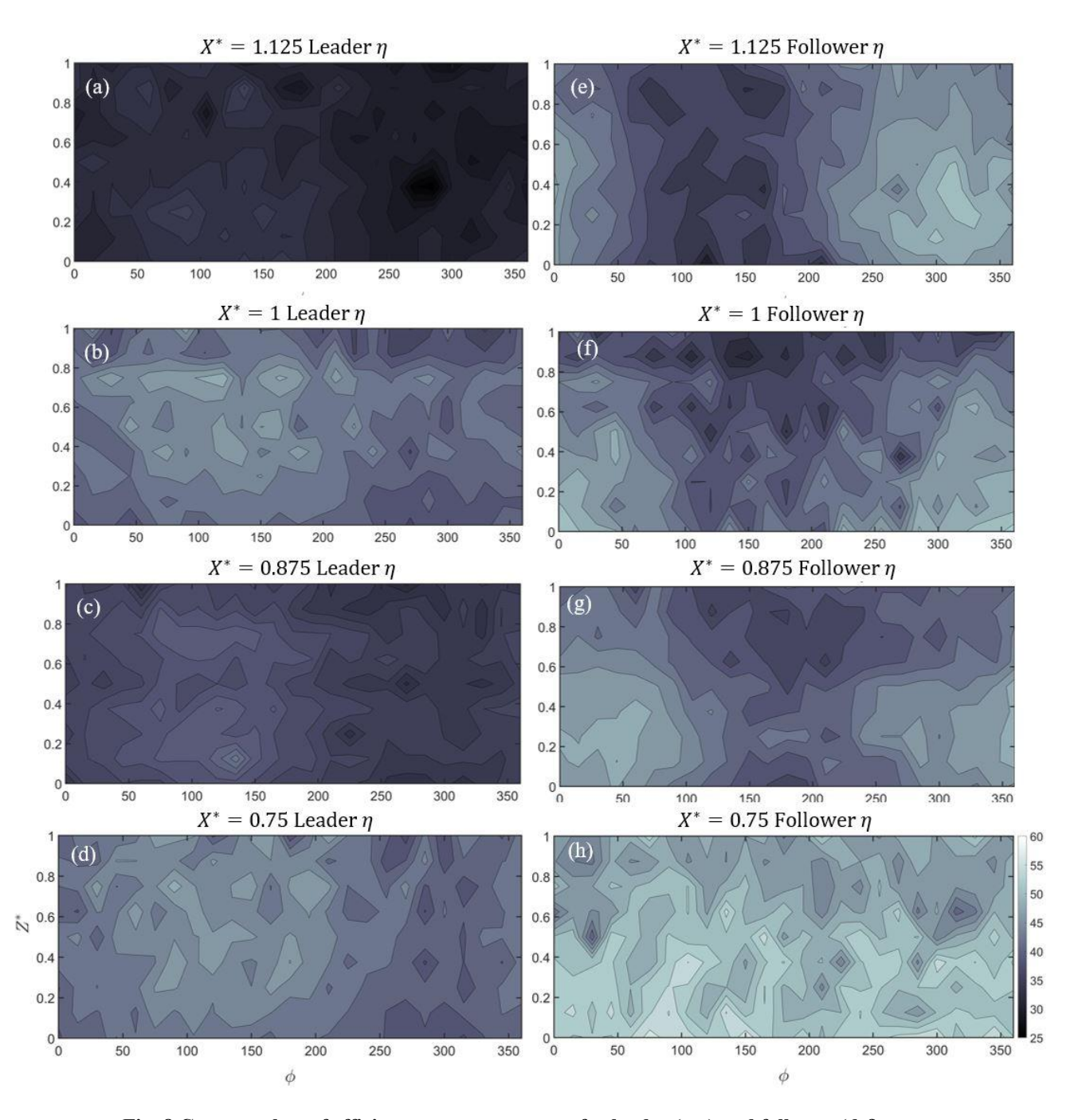


Fig. 8 Contour plots of efficiency, as a percentage, for leader (a-c) and follower (d-f)

# D. Follower behavior in a schooling environment

A summary of the trends in thrust production, power consumption, and propulsive efficiency of the follower hydrofoil for the nearest ( $X^* = 0.75$  chords) and furthest ( $X^* = 1.125$  chords) streamwise spacings is given in Fig. 9. Increasing the spanwise offset ( $Z^*$ ) flattened the sinusoidal power consumption curve, Fig. 9 (a, d), and decreased the peak thrust produced, Fig. 9 (b, e). Decreasing the streamwise spacing increased the phase at which the minimum power consumption occurred, see white regions in Fig. 9 (a, d). The region, highlighted white, corresponds to the minimum thrust production. This minimum thrust production of the follower closely matches that of the leader, see dashed lines in Fig. 9 (b, e). At the largest streamwise spacing tested this region also appears to correspond to an inflection point in the propulsive efficiency of the follower, white region in Fig. 9 (f).

These results suggest that in an unconstrained situation, within the parameter space tested, the follower hydrofoil will always be able to maintain its spacing with the leader while using less power than the leader. However, to accomplish this the follower must modulate its phase offset relative to the leader. This required phase offset is generally unaffected by changes in the spanwise offset, but instead is primarily a function of streamwise spacing. Increases in the spanwise offset did not result in increased power consumption of the follower. Being directly in-line  $(Z^*=0)$  requires the least power input from the follower, but the follower efficiency was always at or higher than the leader. If the follower modulates its phase and moves outside of the low power regions, gray areas in Fig. 9, then it experiences an increase in both power consumption and thrust production. In an unconstrained situation this increased thrust production will serve to push the hydrofoils together in the streamwise direction. Separately, if the follower increases its spanwise offset relative to the leader both power consumption and thrust production. This results in only a small net loss in efficiency (less than 10%) while minimizing the power consumption for the follower.

As the streamwise spacing  $(X^*)$  between the hydrofoils is decreased the minimum thrust, power consumption, and propulsive efficiency increased for both hydrofoils. This suggests that if the phase offset necessary for the hydrofoils to produce identical thrust is maintained, the hydrofoils are likely to accelerate in the streamwise direction and may become more energy efficient. However the minimum power consumption by both hydrofoils will likely still increase due to increases in drag associated with a faster swimming speed.

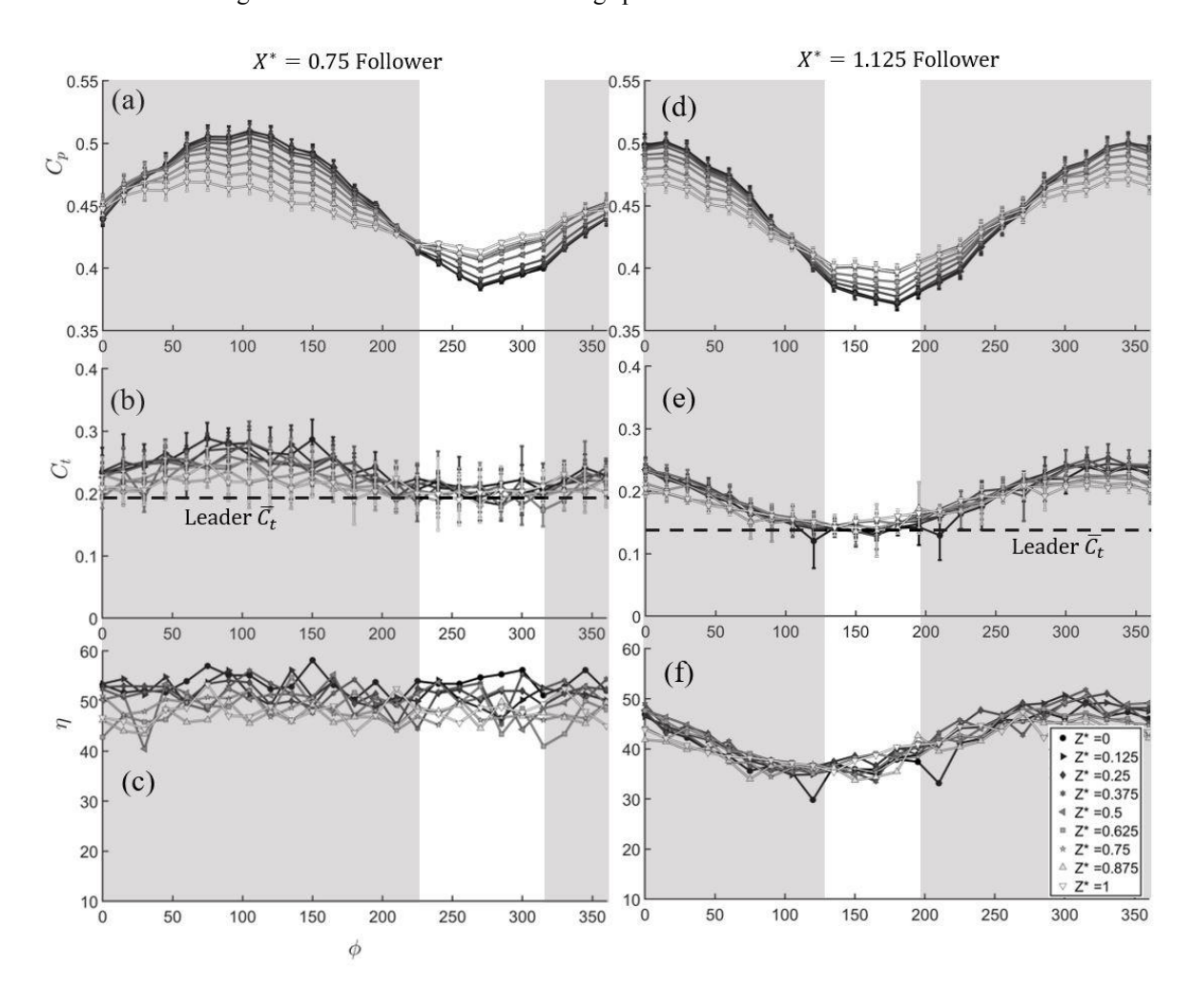


Fig. 9 Power, thrust, and efficiency for follower hydrofoil at two select streamwise spacings.

Thus if the follower wishes to maintain its streamwise spacing with the leader and expend the least energy, it needs to maintain a specific phase, dependent on the streamwise spacing, and zero spanwise offset relative to the leader. If the follower wishes to decrease the streamwise spacing with maximum thrust it needs to maintain zero spanwise offset

and a different phase offset approximately  $170^{\circ}$  below the minimum power phase offset. If the follower wishes to decrease the streamwise spacing with maximum efficiency it needs to stay near  $Z^* = 0.25$  chords relative to the leader. The parameters the follower needs to maintain for these and a number of other actions for  $X^* = 1.125$  chords are summarized in Table 4.

**Table 4** Necessary parameters for follower behaviors at  $X^* = 1.125$  chords

Desired action	Phase offset $(\phi)$	Spanwise Offset $(Z^*)$
Maintain streamwise spacing with minimum power consumption	~185°	0 chords
Decrease streamwise spacing with maximum thrust production	~15°	0 chord
Decrease streamwise spacing with minimum power consumption	~15°	1 chord
Decrease streamwise spacing with maximum propulsive efficiency	~15°	~0.25 chords

## V. Conclusions

An experimental study to investigate the effect of spanwise offset ( $Z^*$ ) in oscillating hydrofoils has been presented. The spanwise offsets tested were found to be neutral equilibrium points in the spanwise direction. As such, there is no inherent fluid dynamic force driving the follower to a particular spanwise offset.

Decreases in the streamwise spacing ( $X^*$ ) between the hydrofoils caused increased thrust production, power consumption, and propulsive efficiency for the leader hydrofoil. The leader hydrofoil only experienced small changes in power consumption with changing phase offset ( $\phi$ ). Increasing the spanwise offset did not significantly alter the thrust production of the leader but did reduce its power consumption.

The thrust produced by the follower hydrofoil never fell below that produced by the leader in all cases tested. The thrust and power consumption of the follower had sine-wave-like shapes with changes in phase offset. At the furthest streamwise spacing tested ( $X^* = 1.125$  chords) the minimum thrust production and power consumption occurred near  $\phi = 185^\circ$ . If the follower hydrofoil modulated its phase offset away from this value it experienced increased thrust production and power consumption. The maximum thrust production and power consumption for the follower occurred near  $\phi = 15^\circ$ . Decreasing the streamwise spacing increased the phase at which these minima and maxima occurred as a result of the convective speed of the incoming vortex street. Increasing the spanwise offset reduced the amplitude of the thrust and power curves. The decrease in power consumption was larger than that in thrust giving increased propulsive efficiency.

These results indicate that neither hydrofoil was negatively impacted by the presence of the other when sufficient streamwise spacing ( $X^* > 0.75$  chords) was maintained. If the hydrofoils are too close together they experience increased unsteady loading. Both hydrofoils experience increased thrust production and propulsive efficiency. This could be beneficial in an unconstrained schooling environment, efficiently increasing the speed at which the school swims. By modulating its phase offset relative to the leader hydrofoil, the follower is able to either maintain or decrease its streamwise spacing relative to the leader. In the case where constant streamwise spacing is desired the follower expends the least energy by staying in-line ( $Z^* = 0$ ) with the leader. In the case where the follower wishes to decrease the streamwise spacing it can increase its efficiency by increasing the spanwise offset with maximum efficiency at near  $Z^* = 0.25$  chords. This information could prove useful for the construction of efficient underwater vehicles propelled by oscillating propulsors.

However, in the parameter space tested, an unconstrained follower is unable to reduce its thrust production below that of the leader through modulation of phase or spanwise offset. This suggests that other factors such as oscillating amplitude or oscillating frequency (Strouhal number) are likely drivers of reducing thrust in this type of alignment. Therefore further investigation of other canonical schooling configurations, oscillating amplitudes, or oscillating frequencies could prove informative.

# Acknowledgments

This work was supported by the National Science Foundation under Program Director Dr. Ronald Joslin in Fluid Dynamics within CBET on NSF CAREER award number 1653181. Research was sponsored by the Army Research Laboratory and was accomplished under Cooperative Agreement Number W911NJ-19-2-0197. The views and conclusions contained in this document are those of the authors and should not be interpreted as representing the official policies, either expressed or implied, of the Army Research Laboratory or the U.S. Government. The U.S. Government is authorized to reproduce and distribute reprints for Government purposes notwithstanding any copyright notation herein.

## References

- [1] Weihs, D. (1973). Hydromechanics of fish schooling. *Nature*, 241, 290–291.
- [2] Portugal, S. J., Hubel, T. Y., Fritz, J., Heese, S., Trobe, D., Voelkl, B., ... Usherwood, J. R. (2014). Upwash exploitation and downwash avoidance by flap phasing in ibis formation flight. *Nature*, *505*, 399–402. https://doi.org/10.1038/nature12939
- [3] Boschitsch, B. M., Dewey, P. A., Smits, A. J., Boschitsch, B. M., Dewey, P. A., & Smits, A. J. (2014). Propulsive performance of unsteady tandem hydrofoils in an in-line configuration. *Physics of Fluids*, 051901. https://doi.org/10.1063/1.4872308
- [4] Dewey, P. A., Quinn, D. B., Boschitsch, B. M., Smits, A. J., Dewey, P. A., Quinn, D. B., & Boschitsch, B. M. (2014). Propulsive performance of unsteady tandem hydrofoils in a side-by-side configuration. *Physics of Fluids*, 26. https://doi.org/10.1063/1.4871024
- [5] Kurt, M., & Moored, K. (2018). Flow Interactions and Performance Benefits in Fish Schools. Bulletin of the American Physical Society, 63.
- [6] Rockwell, D. (1998). VORTEX-BODY INTERACTIONS. Annual Review of Fluid Mechanics, 30, 199-229.
- [7] Garmann, D. J., & Visbal, M. R. (2015). Interactions of a streamwise-oriented vortex with a finite wing. *Journal of Fluid Mechanics*, 767, 782–810. https://doi.org/10.1017/jfm.2015.51
- [8] Garmann, D. J., & Visbal, M. (2016). Further Investigations of the Tip Vortex on an Oscillating NACA0012 Wing. *AIAA Aviation*. https://doi.org/10.2514/6.2016-4343
- [9] Mckenna, C. K., & Rockwell, D. (2016). Topology of vortex wing interaction. *Experiments in Fluids*. https://doi.org/10.1007/s00348-016-2244-3
- [10] Fishman, G., Wolfinger, M., & Rockwell, D. (2017). The structure of a trailing vortex from a perturbed wing. *Journal of Fluid Mechanics*, 824, 701–721. https://doi.org/10.1017/jfm.2017.331
- [11] Mckenna, C. K., Bross, M., & Rockwell, D. (2017). Structure of a streamwise-oriented vortex incident upon a wing. *Journal of Fluid Mechanics*, 816, 306–330. https://doi.org/10.1017/jfm.2017.87
- [12] Cushing, D. H., & Harden Jones, F. R. (1968). Why do Fish School? Nature, 218, 918-920.
- [13] Breder, C. M. (1967). On the Survival Value of Fish Schools. New York Zoological Society, 52–53, 25–40.
- [14] Partridge, B. L., & Pitcher, T. J. (1979). Evidence against a hydrodynamic function for fish schools. *Nature*, 279, 418–419.
- [15] Partridge, B. L., Pitcher, T., Cullen, J. M., & Wilson, J. (1980). The Three-Dimensional Structure of Fish Schools. *Behovioral Ecology and Sociobiology*, 6(4), 277–288.
- [16] Weihs, D. (1973). Hydromechanics of fish schooling. *Nature*, 241, 290–291.

- [17] Weimerskirch, H., Martin, J., Clerquin, Y., Alexandre, P., & Jiraskova, S. (2001). Energy saving in flight formation. *Nature*, 413, 697–698.
- [18] Portugal, S. J., Hubel, T. Y., Fritz, J., Heese, S., Trobe, D., Voelkl, B., ... Usherwood, J. R. (2014). Upwash exploitation and downwash avoidance by flap phasing in ibis formation flight. *Nature*, *505*, 399–402. https://doi.org/10.1038/nature12939